



HAL
open science

Long time evolution of large-scale patterns in a rectangular Rayleigh-Bénard cell

Anne Sergent, Patrick Le Quéré

► **To cite this version:**

Anne Sergent, Patrick Le Quéré. Long time evolution of large-scale patterns in a rectangular Rayleigh-Bénard cell. *Journal of Physics: Conference Series*, 2011, 318 (8), pp.082010. 10.1088/1742-6596/318/8/082010 . hal-04519827

HAL Id: hal-04519827

<https://hal.science/hal-04519827>

Submitted on 25 Mar 2024

HAL is a multi-disciplinary open access archive for the deposit and dissemination of scientific research documents, whether they are published or not. The documents may come from teaching and research institutions in France or abroad, or from public or private research centers.

L'archive ouverte pluridisciplinaire **HAL**, est destinée au dépôt et à la diffusion de documents scientifiques de niveau recherche, publiés ou non, émanant des établissements d'enseignement et de recherche français ou étrangers, des laboratoires publics ou privés.

Long time evolution of large-scale patterns in a rectangular Rayleigh-Bénard cell

A. Sergent^{1,2} & P. Le Quéré¹

¹CNRS, LIMSI, BP 133, 91403, Orsay, France,

²UPMC Univ Paris 06, 75005, Paris, France

E-mail: anne.sergent@limsi.fr

Abstract. The time evolution of the network of quasi-stationary rolls is investigated for the case of a large aspect ratio rectangular Rayleigh-Bénard cell ($A = 5$) by using large eddy simulations. For Rayleigh numbers between 10^7 and 10^{10} , sudden transitions without any external intervention have been observed in all studied cases between two mean flows which are stable on very long time period. During transition, a short reorientation of the rolls axis leads to a flow reversal and an increase in the size of the resulting rolls.

1. Introduction

Rayleigh-Bénard convection is known to present a large variety of coherent flows, which can persist in turbulent regime (Hartlep *et al.*, 2005). The mean large-scale circulation (LSC) generated by the convection can feature metastable flow structures over hundreds or thousands of large eddy turnover times between which spontaneous sudden reversals or changes of direction occur. The abrupt flow reversals and reorientations have been observed experimentally (Xi & Xia, 2008; Brown *et al.*, 2005; Araujo *et al.*, 2005; Sreenivasan *et al.*, 2002; Cioni *et al.*, 1997) and several theoretical models have been proposed for interpreting the dynamic behavior of the LSC (Benzi & Verzicco, 2008; Brown & Ahlers, 2008; Sreenivasan *et al.*, 2002).

From a numerical point of view, few studies concern the reversal and reorientation of the LSC. In a cell with aspect ratio 1/2, Stringano & Verzicco (2006) have observed the flow structure evolving with the Rayleigh number (Ra) from a single roll flow to a flow with two stacked counter-rotating rolls. More recently, P. K. Mishra & Eswaran (2011) have considered the flow in a cylinder of aspect ratio 1 and investigated the flow reversals/reorientations by means of the amplitude and phase of the first azimuthal Fourier modes.

Most of the previously cited experimental or numerical studies have been performed in small aspect ratio containers. But it has been shown numerically in a periodic fluid layer (Hartlep *et al.*, 2005) that up to $Ra = 10^7$ the selected size of circulation cells in turbulent convection increases with Ra in the case of moderate Prandtl numbers (Pr).

The aim of the present work is to study numerically the time evolution of the network of quasi-stationary rolls in a rectangular container of aspect ratio larger than 1. In order to gather data for a significant time period, large eddy simulations are performed. In this paper, we describe the reversal of the LSC in terms of its influence on the global Nusselt number, the flow structure and the Fourier modes.

Table 1. Numerical parameters. $N_x \times N_y \times N_z$ are the number of grid points in each direction, dt : the time step, Δt : the total time of simulation, δ_u and δ_θ : the respective viscous and thermal boundary layer thicknesses obtained from the simulation results, η_h : the ratio of the maximal horizontal grid spacing and the Kolmogorov scale (Grötzbach, 1983), N_{δ_u} and N_{δ_θ} : the respective number of grid points in the viscous and thermal boundary layer thickness.

Rayleigh	$N_x \times N_y \times N_z$	dt	Δt	δ_u	δ_θ	η_h	N_{δ_u}	N_{δ_θ}
$1 \cdot 10^7$	50 x 34 x 130	0.01	30000	0.03434	0.02700	1.7	10	9
$6 \cdot 10^8$	50 x 34 x 130	0.01	60000	0.01740	0.00964	6.7	8	6
$6 \cdot 10^8$	66 x 50 x 194	0.006	12000	0.02009	0.00822	4.5	11	7
$6 \cdot 10^9$	92 x 60 x 240	0.004	10000	0.01369	0.00541	7.5	12	7
$1 \cdot 10^{10}$	100 x 66 x 258	0.003	4000	0.01288	0.00448	8.3	13	7

2. Numerical set-up

Let us consider the air-flow ($Pr = 0.71$) developing in a rectangular cell of moderate aspect ratios (lengths over height L_x , $Ay = L_y/L_x = 1$ and $Az = L_z/L_x = 5$), for Ra ranging from 10^7 to 10^{10} . The fluid is heated from below and cooled from above by two isothermal walls. The four vertical walls are perfectly adiabatic. No-slip boundary condition is applied on the six walls. This geometry corresponds to the experimental rectangular cell studied in Ebert *et al.* (2008).

The 3D Navier-Stokes equations within the Boussinesq approximation have been made dimensionless by using the length L_x , the velocity $\frac{\kappa}{L_x} \sqrt{Ra}$ (where κ is the thermal diffusivity) and the wall temperature difference. The resulting non-dimensional temperature θ varies between -0.5 and 0.5. The governing equations are solved numerically using finite-volume scheme. Details on the numerical methods and on the LES model may be found in Sergent *et al.* (2006). In order to allow the flow structure to re-arrange by itself, no near-wall dynamics (nor the heat transfer) model has been applied.

The code has been validated for the differentially heated cavity (Sergent *et al.*, 2003) and Rayleigh-Bénard convection in a periodic fluid layer (Sergent *et al.*, 2006). In particular, a 2/7 scaling behavior of the heat transfer ($Nu = 0.161Ra^{0.286}$, Nu : Nusselt number) has been reproduced over a large Ra range and a regime transition towards a 1/3 turbulent regime has been observed at $Ra = 2.10^8$.

The spatial resolution used in the present work depends on the Rayleigh number. The numerical parameters are gathered in table 1. Note that these grid criteria are less restrictive than those used in DNS (Stevens *et al.*, 2010). Indeed, the aim of this paper is not to provide accurate solutions but to investigate the temporal evolution of the large scale flow structure over long time period. For this reason, the calculations have been performed over several thousands of large eddy turnover times. In all cases, statistics have been averaged for at least 200 dimensionless time units. To prevent the selection of a particular pattern, all computations have been started from the conductive temperature profile with random noise as initial conditions.

3. Results

3.1. Flow structure

The time series of the temperature at the mid-point of the cavity are presented on figure 1. For all considered Rayleigh numbers (Ra), sudden transition occurs without any external intervention between two mean flows which are stable on very long time period (from $\sim 10^3$ to $\sim 10^4$

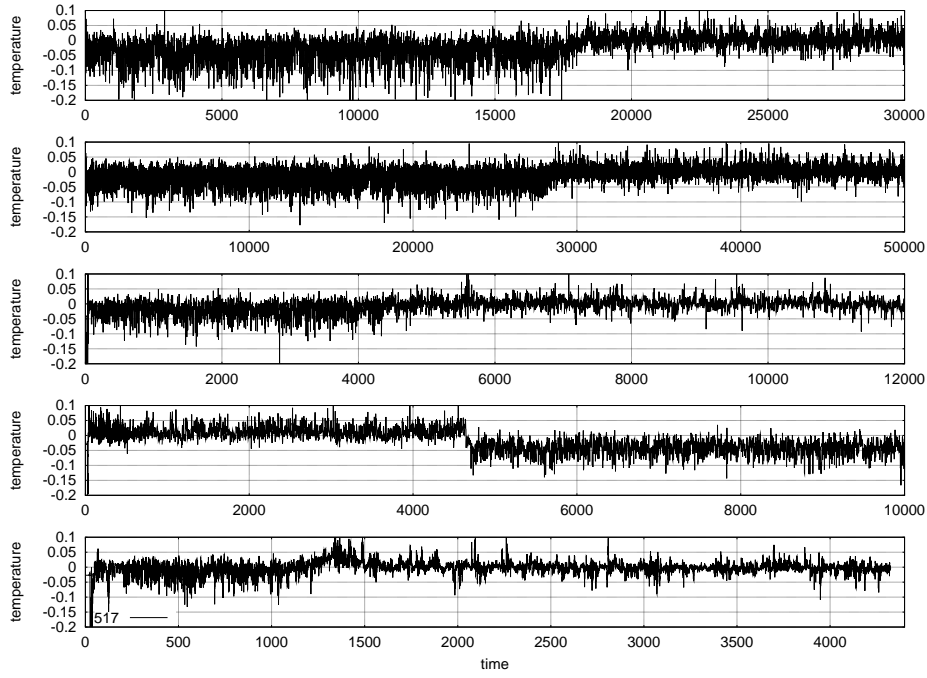


Figure 1. Time series of the temperature at the mid-point $(0.5, 0.5, 2.5)$ for $Ra = 10^7, 6 \cdot 10^8, 6 \cdot 10^9, 10^{10}$ from top to bottom.

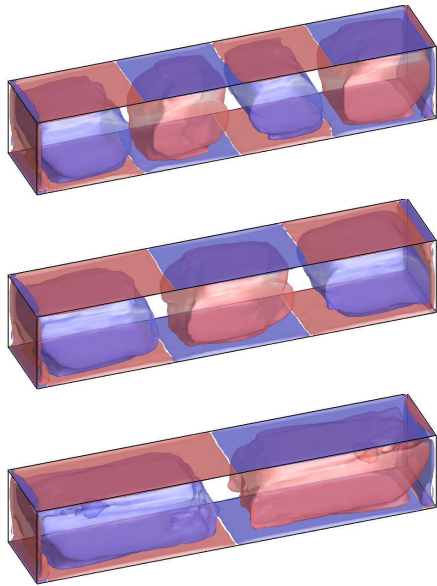


Figure 2. $Ra = 6 \cdot 10^8$. Three different patterns of time-averaged iso-surfaces of y -component of vorticity $\Omega_y = \pm 0.3$.

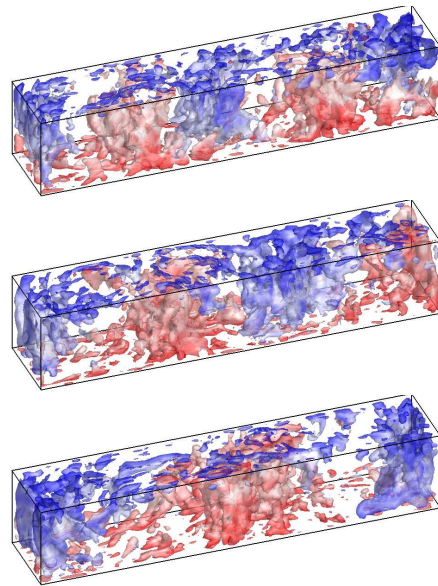


Figure 3. $Ra = 6 \cdot 10^8$. Iso-surfaces of instantaneous vertical heat flux ($\sim 2Nu$), coloured by the temperature field (bottom).

Table 2. Time-averaged Nusselt number at wall and its turbulent convective part at the mid-height ($Nu_t = \sqrt{Ra} \times \langle u'\theta' \rangle$) depending on the flow structure.

Rayleigh	4 rolls	3 rolls	2 rolls
$1 \cdot 10^7$	16.8 (47%)	16.4 (44%)	—
$6 \cdot 10^8$	70.9 (48%)	70.2 (44%)	68.2 (38%)
$6 \cdot 10^9$	137.0 (49%)	—	135.7 (35%)
$1 \cdot 10^{10}$	161.5 (47%)	160.4 (43%)	—

convective time units). In the present work, the first observed mean flow is the same for the four values of Ra . It corresponds to the steady-state solution with 4 counter-rotating rolls placed side by side, on which the background turbulence is superimposed, as shown on figures 2 and 3. The fact that the first flow is independent on Ra demonstrates that the 4-roll flow structure is only transitional before a physical solution is established.

The large coherent flow structures of the second flow correspond to 3 counter-rotating rolls for $Ra = 10^7$ and $6 \cdot 10^8$ and 2 counter-rotating rolls for $Ra = 6 \cdot 10^9$ placed side by side. Only a single large-scale reorganization has been observed in our computations. But due to the long characteristic times, we cannot conclude whether the second observed mean flow is the unique stable state or not. In agreement with results in Hartlep *et al.* (2005); Shishkina & Wagner (2006), it is observed that the spontaneous selected size of the circulation cells increases with Ra for the values of Ra 10^7 , $6 \cdot 10^8$ and $6 \cdot 10^9$. However, at $Ra = 10^{10}$, the second flow corresponds to a 3-rolls structure, which is not consistent with the previous statement. Therefore a second transition may exist at a convective time greater than 4000. Moreover at $Ra = 6 \cdot 10^8$, a 2-rolls flow structure (fig. 2) has been obtained by decreasing Ra from a 2-rolls solution field obtained at higher Ra . This third flow remains stable during at least 10^4 convective times units. Due to the long time period over which the large coherent flow structures can persist with this set of physical parameters, it is not clear whether the 2- and 3- roll flow structures are two possible solution fields, or if the flow will converge eventually towards one of these mean flow configurations.

Table 2 presents the influence of the flow structure on the heat transfer. The global Nusselt number at wall (Nu) (averaged in time and space) decreases slightly with the roll number, whereas the turbulent convective part of the heat transfer at mid-height ($Nu_t(x) = \sqrt{Ra} \langle u'\theta' \rangle$) decreases more significantly. It means that the LSC transitions tend to reduce the fluctuating part of the heat transfer in the cavity bulk.

3.2. LSC reorientation

The reorganization of the large-scale circulation can be described in terms of Fourier transform of the horizontal velocity W in the Z -direction. Hereafter a mode index corresponds to the number of rolls filling the cavity. The figure 4 exhibits the time serie of the amplitude $|W|$ of the four first modes for $Ra = 6 \cdot 10^8$ in a grid point ($X=0.065$, $Y=0.5$) located outside the viscous boundary layer. A sudden transition of the LSC is observed during a short time period (around 50 convective time units). Before transition, the mode 4 dominates the large scales, but the mode 3 already corresponds to the second dominant mode. During the transition, the large scale modes are mixed, but after the transition the mode 3 significantly dominates the other modes. The ratio $|W|_3/|W|_4$ gives rise to the sharp LSC reorganization.

At $Ra = 6 \cdot 10^9$, the mode 4 is replaced by a mode 2 (figure 5). This is in agreement with the (Hartlep *et al.*, 2005) results obtained numerically in a periodic fluid layer, which shows that up

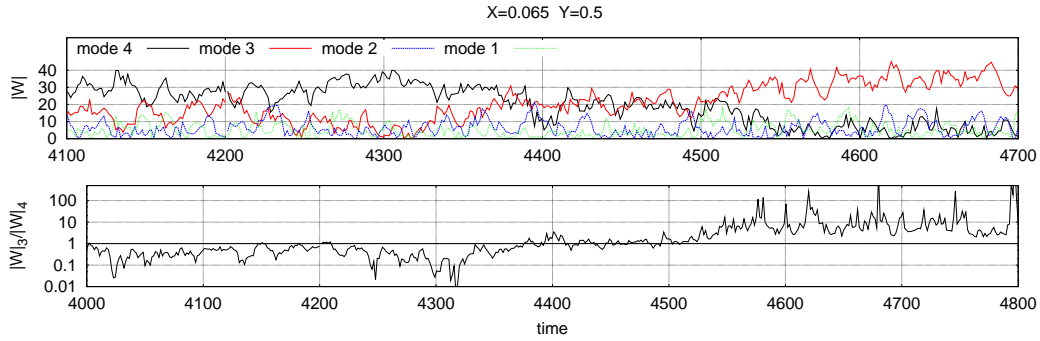


Figure 4. $Ra = 6 \cdot 10^8$: time series of the amplitude ($|W|_i$) of the four first Fourier modes of the horizontal velocity W , where i is the number of rolls contained in the cavity.

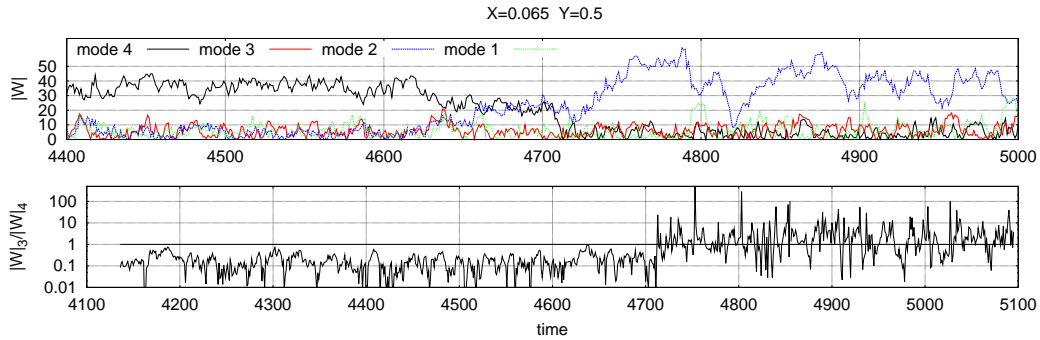


Figure 5. $Ra = 6 \cdot 10^8$: time series of the amplitude ($|W|_i$) of the four first Fourier modes of the horizontal velocity W , where i is the number of rolls contained in the cavity.

to $Ra = 10^7$ the selected size of circulation cells in turbulent convection increases with Ra in the case of moderate Prandtl numbers (Pr).

For $Ra = 10^{10}$, the mode 4 is replaced by the mode 3 (figure 6), but the reorganization is more unclear. The modes 2 and 3 are competing during the transition which takes a longer time (around 350 convective time units). Even after the transition, the mode 2 remains present.

Figure 7 illustrates the reorientation process by use of temporal evolution of the problem variables (θ, U, V, W) along two horizontal lines: one around the edge of the viscous boundary layer and the second at the center of the cavity. We observe that the plumes (θ and U) are well organized over a large part of the cavity, whereas there is no signature of the presence of rolls (V and W) at mid-height. The transition from a 4-rolls flow to a 3-rolls flow, affects all the variables where they are dominated by the LSC. It can be noted that the reorientation process corresponds to the size increase of one of the side rolls. In the same time, the fluid in the remaining part of the cavity flows in the transverse direction (Y), indicating a temporary modification of the rotation axis before establishing a complete mode 3 flow.

4. Concluding remarks

Turbulent thermal convection has been computed by means of Large Eddy Simulation in a rectangular cell of large aspect ratio for Rayleigh numbers between 10^7 and 10^{10} . Sudden

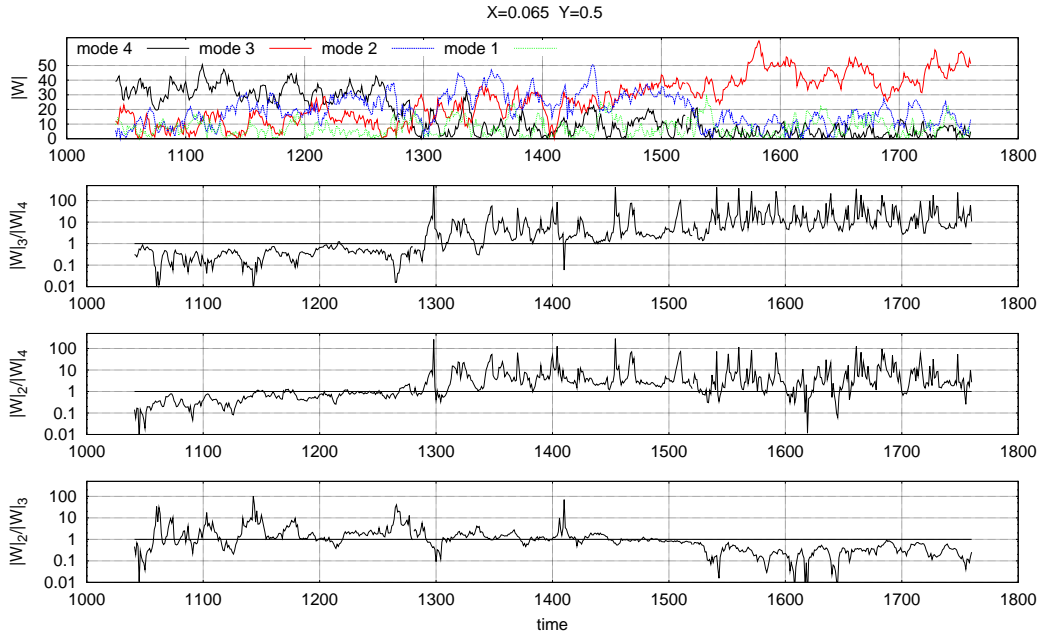


Figure 6. $Ra = 10^{10}$: time series of the amplitude ($|W|_i$) of the four first Fourier modes of the horizontal velocity W , where i is the number of rolls contained in the cavity.

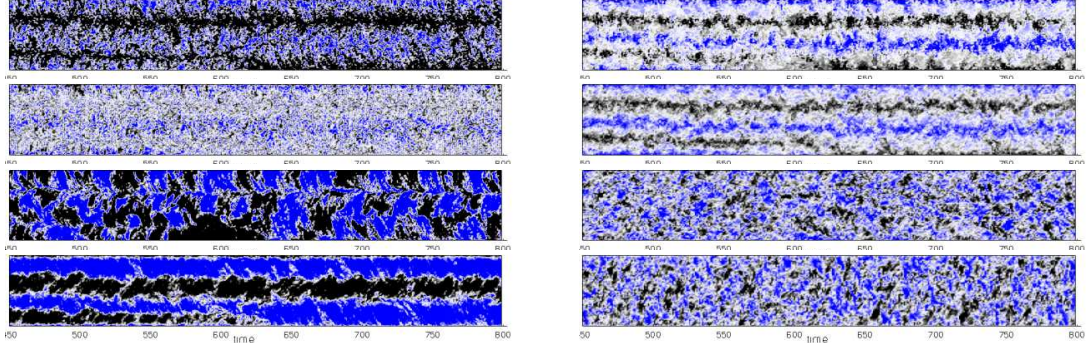


Figure 7. $Ra = 6 \cdot 10^8$. Time evolution of the (θ, U, V, W) variables (from top to bottom) along the horizontal line $(X, 0.5, Z)$ during transition. Left: $X = 0.02$, right: $X = 0.5$

transitions without any external intervention have been observed in all studied cases between two mean flows which are stable on very long time period. During transition, a sharp reorientation of the rolls axis leads to the flow reorientation. The spontaneous selected size of the circulation cells increases with Ra for the values of $Ra = 10^7$, $6 \cdot 10^8$ and $6 \cdot 10^9$. However, at $Ra = 10^{10}$, the transition is more uncertain and the second flow corresponds to a 3-rolls structure, whereas a 2-rolls flow is observed for $Ra = 6 \cdot 10^9$. Due to the long time period over which the large coherent flow structures can persist with this set of physical parameters, it is unclear whether the secondary LSC structure is stable, or if the flow will converge eventually towards new LSC configurations.

Acknowledgments

This work was performed using HPC resources from GENCI-IDRIS (Grant 210326).

References

- ARAÚJO, F. F., GROSSMANN, S. & LOHSE, D. 2005 Wind reversals in turbulent Rayleigh-Bénard convection. *Phys. Rev. Lett.* **95** (8), 084502.
- BENZI, R. & VERZICCO, R. 2008 Numerical simulations of flow reversal in rayleigh-bnard convection. *EPL (Europhysics Letters)* **81** (6), 64008.
- BROWN, E. & AHLERS, G. 2008 A model of diffusion in a potential well for the dynamics of the large-scale circulation in turbulent rayleighbnard convection **20**, 075101.
- BROWN, E., NIKOLAENKO, A. & AHLERS, G. 2005 Reorientation of the large-scale circulation in turbulent Rayleigh-Bénard convection. *Phys. Rev. Lett.* **95**, 084503.
- CIONI, S., CILIBERTO, S. & SOMMERIA, J. 1997 Strongly turbulent rayleighbnard convection in mercury: comparison with results at moderate prandtl number. *J. Fluid Mech.* **335**, 111–140.
- EBERT, A., RESAGK, C. & THESS, A. 2008 Experimental study of temperature distribution and local heat flux for turbulent Rayleigh-Bénard convection of air in a long rectangular enclosure. *Int. J. Heat Mass Trans.* **51**, 4238–4248.
- GRÖTZBACH, G. 1983 Spatial resolution requirements for direct numerical simulation of the Rayleigh-Bénard convection **49**, 241–264.
- HARTLEP, T., TILGNER, A. & BUSSE, F.H. 2005 Transition to turbulent convection in a fluid layer heated from below at moderate aspect ratio. *J. Fluid Mech.* **554**, 309–322.
- P. K. MISHRA, A. K. DE, M. K. VERMA & ESWARAN, V. 2011 Dynamics of reorientations and reversals of large-scale flow in rayleighbnard convection. *J. Fluid Mech.* **668**, 480–499.
- SERGENT, A., JOUBERT, P. & QUÉRÉ, P. LE 2003 Development of a local subgrid diffusivity model for large eddy simulation of buoyancy driven flows: application to a square differentially heated cavity. *Num. Heat Trans. A* **44**, 789–810.
- SERGENT, A., JOUBERT, P. & QUÉRÉ, P. LE 2006 Large eddy simulation of Rayleigh-Bénard convection in an infinite plane channel using a mixed scale diffusivity model. *P. Comp. Fluid Dyn.* **6**, 40–49.
- SHISHKINA, O. & WAGNER, C. 2006 Analysis of thermal dissipation rates in turbulent Rayleigh-Bénard convection. *J. Fluid Mech.* **546**, 51–60.
- SREENIVASAN, K. R., BERSHADSKII, A. & NIEMELA, J. J. 2002 Mean wind and its reversal in thermal convection. *Phys. Rev. E* **65** (5), 056306.
- STEVENS, R. J. A. M., VERZICCO, R. & LOHSE, D. 2010 Radial boundary layer structure and Nusselt number in RayleighBénard convection. *J. Fluid Mech.* **643**, 495–507.
- STRINGANO, G. & VERZICCO, R. 2006 Mean flow structure in thermal convection in a cylindrical cell of aspect ratio one half. *J. Fluid Mech.* **548**, 1–16.
- XI, H.D. & XIA, K.Q. 2008 Flow mode transitions in turbulent thermal convection. *Phys. Fluids* **20**, 055104.